

# Hybrid Rylene Arrays via Combination of Stille Coupling and C–H Transformation as High-Performance Electron Transport Materials

Wan Yue,<sup>†,‡</sup> Aifeng Lv,<sup>†,‡</sup> Jing Gao,<sup>†,‡</sup> Wei Jiang,<sup>†</sup> Linxiao Hao,<sup>†,‡</sup> Cheng Li,<sup>†,‡</sup> Yan Li,<sup>\*,†</sup> Lauren E. Polander,<sup>§</sup> Stephen Barlow,<sup>§</sup> Wenping Hu,<sup>†</sup> Simone Di Motta,<sup>||</sup> Fabrizia Negri,<sup>\*,||</sup> Seth R. Marder,<sup>\*,§</sup> and Zhaohui Wang<sup>\*,†</sup>

<sup>†</sup>Beijing National Laboratory for Molecular Science, Key Laboratory of Organic Solids, Institute of Chemistry, Chinese Academy of Sciences, Beijing 100190, China

<sup>‡</sup>Graduate School of the Chinese Academy of Sciences, Beijing 100190, China

<sup>§</sup>School of Chemistry and Biochemistry and Center for Organic Photonics and Electronics, Georgia Institute of Technology, 901 Atlantic Drive NW, Atlanta, Georgia 30332-0400, United States

<sup>||</sup>Dipartimento di Chimica “G. Ciamician”, Università di Bologna, Via F. Selmi 2, 40126 Bologna, Italy, and INSTM, UdR Bologna, Italy

**S** Supporting Information

**ABSTRACT:** Hybrid rylene arrays have been prepared via a combination of Stille coupling and C–H transformation. The ability to extend the  $\pi$  system along the equatorial axis of rylenes not only leads to broadened light absorption but also increases the electron affinity, which can facilitate electron injection and transport with ambient stability.

The design, synthesis, and characterization of new high-performance organic semiconductors are important for the development of next-generation optoelectronic devices.<sup>1</sup> To date, there has been a tremendous effort to narrow the gap in performance (ambient stability, mobility, etc.) between organic semiconductors with n-channel field-effect transistor (FET) behavior and their leading p-channel counterparts. Naphthalene tetracarboxylic diimides (NDIs) and perylene tetracarboxylic diimides (PDIs) are among the most promising building blocks for achieving this challenging goal.<sup>2</sup> We became interested in examining hybrid rylene arrays formed by lateral fusion of PDIs and NDIs, since they could possibly lead to materials that would have broad absorption and high electron affinity (EA) and, depending on the substitution on the nitrogen atoms, could be processable and have a strong tendency to  $\pi$ -stack.<sup>3,4</sup>

We are particularly interested in the design and synthesis of novel  $\pi$ -extended electron-poor molecules based on rylene diimides with unique optoelectronic properties. Recently, some of us reported the facile homocoupling of tetrahalogenated PDIs to give triply linked oligo-PDIs via Ullmann reaction and C–H transformation<sup>5</sup> and its use in obtaining a series of functionalized graphene-ribbon-type molecules.<sup>6</sup> Quite recently, tetracene tetracarboxylic diimides have also been synthesized via direct double ring extension of electron-deficient NDIs involving metallacyclopentadienes.<sup>7</sup> Herein we present a facile one-pot synthesis of a new family of hybrid rylene diimide arrays (3, Figure 1) via a combination of Stille coupling and C–H transformation. In general, successful extension of the  $\pi$  system along the equatorial axis of rylenes

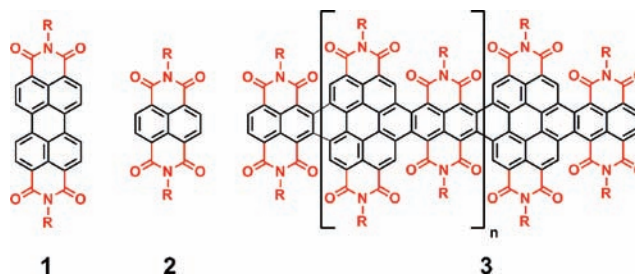


**Figure 1.** Perylene diimides 1, naphthalene diimides 2, and hybrid rylene arrays 3.

can lead to increased optical absorption and in particular to higher EA, facilitating electron injection and increasing the possibility of transport with ambient stability, although there are exceptions (e.g., expansion of perylene diimides to coronene diimides leads to blue-shifted absorption and increased LUMO energies).<sup>8</sup> Indeed, the hybrid rylene arrays exhibit excellent organic thin-film transistor (OTFT) characteristics under ambient conditions.

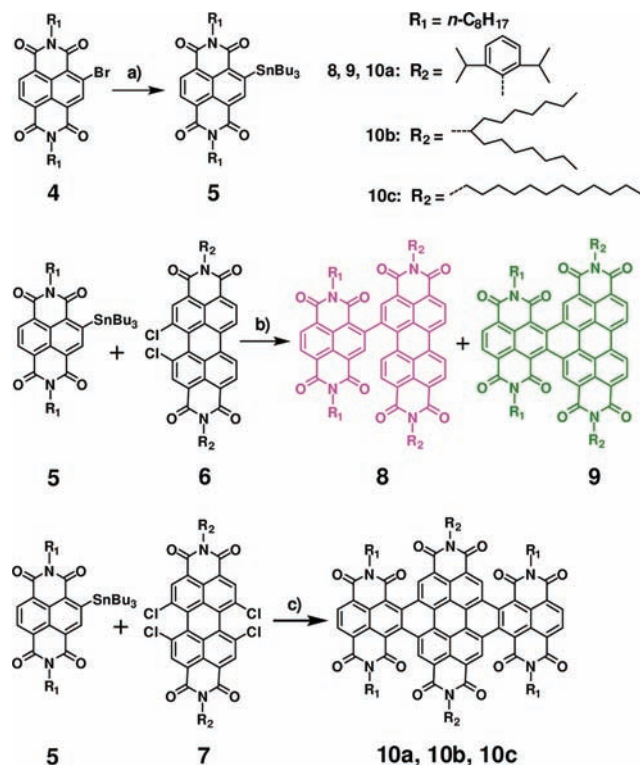
Stille cross-couplings have proved to be an especially popular tool for carbon–carbon bond formation because of the air and moisture stability of organotin reagents as well as the excellent functional group compatibility.<sup>9</sup> Trialkyltin derivatives are usually obtained from halogen-substituted aromatics via halogen–lithium exchange followed by reaction of the lithium intermediate with trialkyltin chloride.<sup>10</sup> Since NDIs and PDIs are not stable toward alkyllithiums, this approach is not applicable, and until recently, their tin derivatives have remained hypothetical. However, some of us have recently reported that mono- and distannyl NDI derivatives can be obtained by coupling of the corresponding mono- and dibromo derivatives with  $\text{Bu}_3\text{Sn–SnBu}_3$  in the presence of  $\text{Pd}_2(\text{dba})_3$  and  $\text{P}(o\text{-tol})_3$  in toluene.<sup>11</sup> The same procedure was used to

**Received:** February 6, 2012

**Published:** March 21, 2012

synthesize the 2-tributyltin- and  $N,N'$ -dioctyl-substituted NDI **5** (Scheme 1).

### Scheme 1. Synthesis of Hybrid Rylene Arrays<sup>a</sup>



<sup>a</sup>Conditions: (a)  $\text{Pd}_2(\text{dba})_3$ ,  $\text{P}(o\text{-tol})_3$ ,  $\text{Bu}_3\text{Sn-SnBu}_3$ , toluene, reflux; (b)  $\text{Pd}(\text{PPh}_3)_4$ ,  $\text{CuI}$ , toluene, reflux; (c)  $\text{Pd}(\text{PPh}_3)_4$ , toluene, reflux. Yields: **5** (80%), **8** (25%), **9** (33%), **10a** (46%), **10b** (40%), and **10c** (35%).

Inspired by the previous creation of fused aromatic rings via Ullmann reaction and C–H transformation, we envisaged that the cross-coupling of this key intermediate **5** with halogenated PDIs would provide a straightforward and promising method for construction of fused hybrid NDI–PDI arrays via Stille coupling and C–H transformation. Accordingly, 1,2-dichlorinated perylene diimide **6**<sup>12</sup> was chosen as model substrate; cross-coupling with **5** using  $\text{Pd}(\text{PPh}_3)_4$  and  $\text{CuI}$  remarkably afforded singly linked and doubly linked compounds, named singly linked NDI–PDI **8** and hybrid NDI–PDI array **9**, respectively. Encouraged by the success of this annulation, we used readily available 1,6,7,12-tetrachloro perylene diimides **7** to check the scope of our procedure. By this method, different substituents can be conveniently introduced into the extended hybrid NDI–PDI–NDI array **10**.

Because of the steric encumbrance effect involving the oxygen atoms of the NDI and the neighboring hydrogens of the PDI, the B3LYP/6-31G\*–optimized geometries of **9** and **10** predict their cores to be markedly nonplanar, while the NDI and PDI units in the singly linked array **8** are found to be almost perpendicular (see Figures S1–S3 in the Supporting Information). Similarly to PDI arrays,<sup>5d</sup> the heliciform and nonheliciform structures correspond to the lowest-energy conformers of **9** and **10** (see Table S1).

As we expected, the hybrid rylene arrays show broad absorption with high absorptivity over much of the visible region, suggesting the possible application of these arrays as

active layers in organic photovoltaic cells.<sup>13</sup> The absorption spectrum of the singly linked NDI–PDI compound **8** is essentially a superposition of those of the NDI and PDI units (380 and 527 nm, respectively; Figure 2), suggesting weak

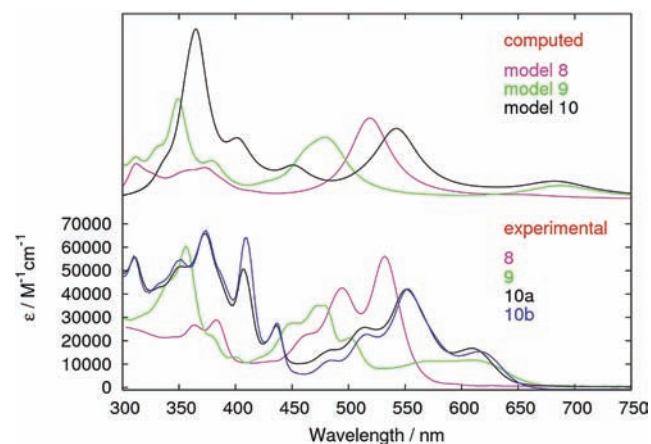


**Figure 2.** UV–vis absorption spectra of hybrid rylene arrays **8** (magenta), **9** (green), **10a** (black), and **10b** (blue) in chloroform (bottom) and a comparison with the corresponding TDDFT/6-31G\*–computed spectra not including vibronic structures (top).

communication between the NDI and PDI, as implied by the significant computed twist angle between the two rylene units (see Figure S1). This conclusion is further supported by a comparison of the computed absorption spectra of the NDI, the PDI, and **8** (see Figure S4). In contrast, the absorption spectra of the doubly linked hybrid NDI–PDI and NDI–PDI–NDI arrays are more complicated, with low-energy maxima bathochromically shifted to ca. 610 nm (Figure 2). An analysis in terms of the orbital nature of the TD-B3LYP/6-31G\*–computed electronic transitions of **9** and **10** sheds more light on the nature of the lowest-energy transitions. As shown in Figure 3, the HOMOs of the arrays are mainly localized on the PDI unit, while the LUMOs are mainly localized on the NDI unit(s). As a result, the weak lowest-energy transition, which is dominated by the HOMO → LUMO excitation, displays some charge-transfer character (see Figure S6), which is also the

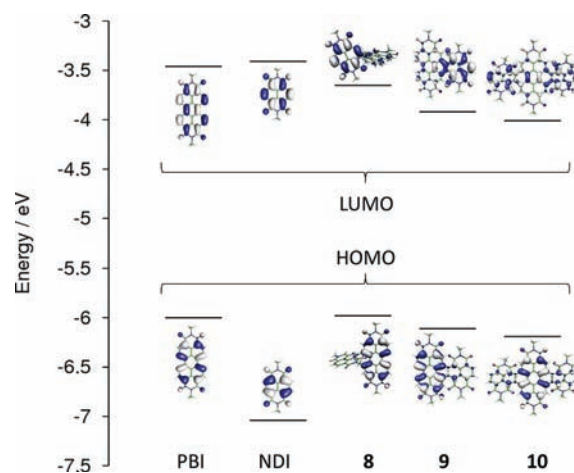


**Figure 3.** Energies and shapes of B3LYP/6-31G\* frontier orbitals (HOMOs and LUMOs) of model PDI, NDI, **8**, **9**, and **10**, showing the dominant orbital parentage across the hybrid rylene arrays.

origin of the underestimation of its energy at the TD-B3LYP/6-31G\* level. The next transition, which has a higher intensity, deserves a comment, since its energy decreases considerably in going from **9** (ca. 480 nm) to **10** (ca. 550 nm). This band is dominated by a  $\pi \rightarrow \pi^*$  electronic excitation to the LUMO from an occupied orbital bearing the same parentage for **9** and **10**. The occupied  $\pi$  orbital is highly delocalized on the extended  $\pi$  core (see Figures S7–S8) since it results from PDI and NDI orbitals that have suitable energy and shape to mix strongly. Therefore, the energy of this transition decreases remarkably with the extension of the aromatic core by fusion of NDI and PDI units.

The redox properties of these hybrid rylene arrays were investigated by cyclic voltammetry in dichloromethane (vs Ag/AgCl). The half-wave reduction potentials of the representative compounds are  $-0.63$  and  $-1.11$  V for NDI;  $-0.56$  and  $-0.82$  V for PDI;  $-0.49$ ,  $-0.64$ ,  $-0.88$ , and  $-1.17$  V for singly linked NDI–PDI **8**;  $-0.19$ ,  $-0.52$ ,  $-1.14$ , and  $-1.38$  V for hybrid NDI–PDI array **9**; and  $-0.16$ ,  $-0.35$ ,  $-0.63$ , and  $-0.84$  V for hybrid NDI–PDI–NDI array **10a**. The first reduction potentials of these hybrid rylene arrays are much less negative than those of parent the NDI and PDI (Table 1), indicating

**Table 1. Optoelectronic Properties and Energy Levels of Hybrid Rylene Arrays**

	$\lambda_1$ (nm) <sup>a</sup>	$E_{1r}$ (V) <sup>b</sup>	EA (eV) <sup>c</sup>	IP (eV) <sup>d</sup>	$E_g$ (eV) <sup>e</sup>
NDI <sup>f</sup>	380	$-0.63$	3.90	7.02	3.12
PDI <sup>g</sup>	527	$-0.56$	3.91	6.21	2.30
<b>8</b>	532	$-0.49$	3.98	6.19	2.21
<b>9</b>	608	$-0.19$	4.24	6.10	1.86
<b>10a</b>	610	$-0.16$	4.28	6.20	1.92
<b>10b</b>	614	$-0.20$	4.26	6.16	1.90
<b>10c</b>	613	$-0.12$	4.35	6.25	1.90

<sup>a</sup>Peak in the visible region. <sup>b</sup>Half-wave redox potential (in V vs Ag/AgCl) measured in CH<sub>2</sub>Cl<sub>2</sub> at a scan rate of 0.1 V/s with ferrocene as an internal potential marker. <sup>c</sup>Estimated from the onset potential of the first reduction wave. <sup>d</sup>Ionization potential estimated from the EA and  $E_g$ . <sup>e</sup>Band-gap energy obtained from the edge of the absorption spectrum. <sup>f</sup>NDI: *N,N'*-di-*n*-octylnaphthalene-1,2:6,7-tetracarboxylic acid diimide. <sup>g</sup>PDI: *N,N'*-bis(2,6-diisopropylphenyl)perylene-3,4,9,10-tetracarboxylic acid diimide.

that they are considerably stronger electron acceptors. The EAs of these compounds were estimated from the onset potentials of the first reduction waves; those of the fused arrays are all in excess of 4.2 eV, meeting the criterion for achieving air-stable electron transport.<sup>3b,4c</sup>

Thin films of the hybrid rylene array **10b** with thicknesses of 40–60 nm were spin-coated from a chloroform solution onto octadecyltrichlorosilane-treated SiO<sub>2</sub>/Si substrates. Gold electrodes with width/length of 1 mm/0.05 mm were applied on the organic thin films through a shadow mask, affording a bottom-gate top-contact device configuration. All devices were tested under ambient conditions. The unannealed thin-film devices showed a moderate electron mobility of 0.02 cm<sup>2</sup> V<sup>-1</sup> s<sup>-1</sup>. Thermal annealing of the thin films led to a substantial improvement in the device performance. The highest electron mobility (0.25 cm<sup>2</sup> V<sup>-1</sup> s<sup>-1</sup>) was achieved after annealing at 220 °C and was accompanied by a high current on/off ratio of 10<sup>7</sup> (Figure 4).

In summary, a new family of hybrid rylene arrays has been prepared via a combination of Stille coupling and C–H

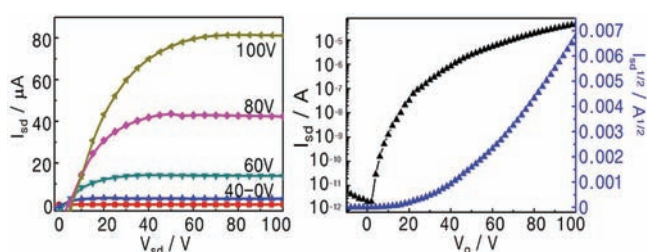


**Figure 4.** (left) Output and (right) transfer characteristics of organic FETs consisting of thin films of hybrid rylene array **10b** with a mobility of 0.25 cm<sup>2</sup> V<sup>-1</sup> s<sup>-1</sup> and an on/off ratio of 10<sup>7</sup>.

transformation. The success of  $\pi$ -system extension along the equatorial axis of rylene not only leads to a dramatically broadened absorption spectrum but also increases the electron affinities to facilitate electron injection and transport with ambient stability. One of these hybrid rylene arrays exhibits excellent OTFT characteristics under ambient conditions.

## ■ ASSOCIATED CONTENT

### 📄 Supporting Information

Experimental details and characterization data for all new compounds; absorption spectrum of hybrid rylene array **10c**; cyclic voltammograms of hybrid rylene arrays **8**, **9**, and **10**; and computational details and additional computational results. This material is available free of charge via the Internet at <http://pubs.acs.org>.

## ■ AUTHOR INFORMATION

### Corresponding Author

yanli@iccas.ac.cn; fabrizia.negri@unibo.it; seth.marder@chemistry.gatech.edu; wangzhaohui@iccas.ac.cn

### Notes

The authors declare no competing financial interest.

## ■ ACKNOWLEDGMENTS

For financial support of this research, we thank the National Natural Science Foundation of China (91027043, 21190032, 20721061), the 973 Program (2011CB932301, 2012CB932903), NSFC–DFG Joint Project TRR61, Solvay, the Chinese Academy of Sciences, the STC Program of the National Science Foundation (DMR-0120967), and Italian PRIN 2008, Project JKBBK4.

## ■ REFERENCES

- (1) (a) Facchetti, A. *Mater. Today* **2007**, *10*, 28. (b) Usta, H.; Facchetti, A.; Marks, T. J. *Acc. Chem. Res.* **2011**, *44*, 501.
- (2) For recent reviews, see: (a) Würthner, F.; Stolte, M. *Chem. Commun.* **2011**, 47, 5109. (b) Huang, C.; Barlow, S.; Marder, S. R. *J. Org. Chem.* **2011**, *76*, 2386. (c) Weil, T.; Vosch, T.; Hofkens, J.; Peneva, K.; Müllen, K. *Angew. Chem., Int. Ed.* **2010**, *49*, 9068.
- (3) (a) Jones, B. A.; Ahrens, M. J.; Yoon, M.-H.; Facchetti, A.; Marks, T. J.; Wasielewski, M. R. *Angew. Chem., Int. Ed.* **2004**, *43*, 6363. (b) Gsänger, M.; Oh, J. H.; Könemann, M.; Höffken, H. W.; Krause, A.-M.; Bao, Z.; Würthner, F. *Angew. Chem., Int. Ed.* **2010**, *49*, 740. (c) Schmidt, R.; Oh, J. H.; Sun, Y.-S.; Deppisch, M.; Krause, A.-M.; Radacki, K.; Braunschweig, H.; Könemann, M.; Erk, P.; Bao, Z.; Würthner, F. *J. Am. Chem. Soc.* **2009**, *131*, 6215.
- (4) (a) Guo, X.; Watson, M. D. *Org. Lett.* **2008**, *10*, 5333. (b) Yan, H.; Chen, Z.; Zheng, Y.; Newman, C.; Quinn, J. R.; Dötz, F.; Kastler, M. *Nature* **2009**, *457*, 679. (c) Jones, B. A.; Facchetti, A.; Wasielewski, M. R.; Marks, T. J. *J. Am. Chem. Soc.* **2007**, *129*, 15259. (d) Katz, H. E.; Lovinger, A. J.; Johnson, J.; Kloc, C.; Siegrist, T.; Li, W.; Lin, Y.-Y.



Dodabalapur, A. *Nature* **2000**, *404*, 478. (e) Thalacker, C.; Röger, C.; Würthner, F. *J. Org. Chem.* **2006**, *71*, 8098. (f) Gao, X.; Di, C.; Hu, Y.; Yang, X.; Fan, H.; Zhang, F.; Liu, Y.; Li, H.; Zhu, D. *J. Am. Chem. Soc.* **2010**, *132*, 3697. (g) Hu, Y.; Gao, X.; Di, C.; Yang, X.; Zhang, F.; Liu, Y.; Li, H.; Zhu, D. *Chem. Mater.* **2011**, *23*, 1204.

(5) (a) Qian, H.; Wang, Z.; Yue, W.; Zhu, D. *J. Am. Chem. Soc.* **2007**, *129*, 10664. (b) Qian, H.; Yue, W.; Zhen, Y.; Di Motta, S.; Di Donato, E.; Negri, F.; Qu, J.; Xu, W.; Zhu, D.; Wang, Z. *J. Org. Chem.* **2009**, *74*, 6275. (c) Shi, Y.; Qian, H.; Li, Y.; Yue, W.; Wang, Z. *Org. Lett.* **2008**, *10*, 2337. (d) Qian, H.; Negri, F.; Wang, C.; Wang, Z. *J. Am. Chem. Soc.* **2008**, *130*, 17970. (e) Zhen, Y.; Wang, C.; Wang, Z. *Chem. Commun.* **2010**, *46*, 1926.

(6) (a) Wu, Y.; Zhen, Y.; Ma, Y.; Zheng, R.; Wang, Z.; Fu, H. *J. Phys. Chem. Lett.* **2010**, *1*, 2499. (b) Wang, H.; Su, H.; Qian, H.; Wang, Z.; Wang, X.; Xia, A. *J. Phys. Chem. A* **2010**, *114*, 9130.

(7) (a) Yue, W.; Gao, J.; Li, Y.; Jiang, W.; Di Motta, S.; Negri, F.; Wang, Z. *J. Am. Chem. Soc.* **2011**, *133*, 18054. (b) Katsuta, S.; Tanaka, K.; Maruya, Y.; Mori, S.; Masuo, S.; Okujima, T.; Uno, H.; Nakayama, K.; Yamada, H. *Chem. Commun.* **2011**, *47*, 10112. (c) Suraru, S.-L.; Zschieschang, U. Z.; Klauk, H.; Würthner, F. *Chem. Commun.* **2011**, *47*, 11504.

(8) (a) Rohr, U.; Schlichting, P.; Böhm, A.; Gross, M.; Meerholz, K.; Bräuchle, C.; Müllen, K. *Angew. Chem., Int. Ed.* **1998**, *37*, 1434. (b) Adachi, M.; Nagao, Y. *Chem. Mater.* **2001**, *13*, 662. (c) Eversloh, C. L.; Li, C.; Müllen, K. *Org. Lett.* **2011**, *13*, 4148. (d) Li, Y.; Xu, L.; Liu, T.; Yu, Y.; Liu, H.; Li, Y.; Zhu, D. *Org. Lett.* **2011**, *13*, 5692.

(9) (a) Kosugi, M.; Sasazawa, K.; Shimizu, Y.; Migita, T. *Chem. Lett.* **1977**, *301*. (b) Milstein, D.; Stille, J. K. *J. Am. Chem. Soc.* **1978**, *100*, 3636.

(10) (a) Littke, A. F.; Schwarz, L.; Fu, G. C. *J. Am. Chem. Soc.* **2002**, *124*, 6343. (b) Zhang, L.; Tan, L.; Hu, W.; Wang, Z. *J. Mater. Chem.* **2009**, *19*, 8216.

(11) Polander, L. E.; Romanov, A. S.; Barlow, S.; Hwang, D. K.; Kippelen, B.; Timofeeva, T. V.; Marder, S. R. *Org. Lett.* **2012**, *14*, 918.

(12) Zhen, Y.; Qian, H.; Xiang, J.; Qu, J.; Wang, Z. *Org. Lett.* **2009**, *11*, 3084.

(13) Li, C.; Wonneberger, H. *Adv. Mater.* **2012**, *24*, 613.